Application of Interpolating Moving Least Squares Fitting to Hypervelocity Collision Dynamics: $O(^3P) + HCl$[†]

Jon P. Camden*

Department of Chemistry, University of Tennessee, Knoxville, Tennessee 37996-1600

Richard Dawes* and Donald L. Thompson

Department of Chemistry, University of Missouri−Columbia, Columbia, Missouri 65211

Received: December 22, 2008; Revised Manuscript Received: February 5, 2009

We use an automated interpolating moving least-squares (IMLS) algorithm, which generates a fitted ab initio surface for systems of arbitrary topology, to construct a global OHCl ($^3A''$) surface at the UB3LYP/aug-cc-pVTZ level of theory. This analytic PES includes all reaction channels and OHCl geometries with energies up to 144 kcal/mol (6.25 eV) above the O + HCl asymptote. The fitted surface was combined with the quasiclassical trajectory method to study the dynamics of the $O(^3P)$ + HCl reaction at hyperthermal collision energies. The fitted PES greatly improves energy conservation during trajectory integration and eliminates problems with ab initio convergence, which are often encountered during direct dynamics studies. The more extensive trajectory calculations yield new insight into the title reaction and agree well with previous experimental studies and direct dynamics results.

I. Introduction

Hyperthermal collisions play an important role in the chemistry of extreme environments, such as those encountered in plasmas, rocket plumes, and space vehicles in low-earth orbit.[1] While our understanding of hyperthermal chemistry is still much less detailed than the chemistry of thermal reactions, recent efforts[2−5] are beginning to elucidate the unique features of hyperthermal collisions. The energy available in these collisions often exceeds several reaction barriers and thus provides access to multiple reaction pathways. Predicting product branching ratios and reaction mechanisms for hyperthermal reactions is a challenging task because it requires an accounting of both energetic and dynamical features. For example, in the reaction of H_2O with hyperthermal $O(^3P)$ the energetically accessible $H_2 + O_2$ product channel is not observed because of dynamical restrictions imposed by the collision geometry.[4] The O + HCl system explored here is of particular interest. Recent simulations by Gimelshein et al.[6] have shown that hyperthermal O + HCl chemistry plays an important role in the reacting flows that result from the interaction of a jet aircraft and the rarefied atmosphere found at high altitudes. Their study illustrates the need for accurate reaction cross sections and product branching ratios over a wide range of collision energies.

The reactions of hyperthermal $O(^3P)$ have been of particular interest because of their importance for spacecraft and rockets in low-earth orbit.[7] A combination of molecular beam scattering techniques and quasiclassical trajectory (QCT) calculations have been employed by the Schatz and Minton groups to study the reactions of $O(^3P)$ with small molecules.[8−11] One major challenge in performing QCT studies on these systems is the development of a full dimensional potential energy surface (PES). While the practice of generating fitted ab initio surfaces is standard for systems of only a few atoms, it is often time-consuming, especially when trying to survey a large number of reactive systems. Further, methods which only treat a region of the surface or selected product channels are not desirable because one does not know a priori which channels will be populated. Therefore, previous studies employed direct dynamics calculations where the energies and gradients are generated on-the-fly at the semiempirical or density functional level of theory. Direct dynamics calculations avoid the task of generating a full dimensional PES, which may be challenging or even impractical; unfortunately, because the many-body electronic structure problem must be solved several times for each integration time step it is computationally costly and therefore limited to lower levels of theory. Nevertheless, previous studies have found qualitative and sometimes quantitative agreement between trajectory studies and molecular beam experiments illustrating the applicability of this approach. When a detailed study of one reaction or a survey of a large number of reactions is required, for example when trying to understand the complex chemistry of a rocket plume where many different reactions carry importance, direct dynamics is not feasible. In this work, we demonstrate that the combination of interpolating moving least-squares (IMLS) fitting[12−14] with trajectory calculations yields a more comprehensive and accurate trajectory study than is possible with direct dynamics. The IMLS-based automatic surface generation algorithm allows construction of fitted PESs for systems with arbitrary topologies in a black-box fashion. This approach therefore utilizes the speed and accuracy associated with a fitted analytical surface while reducing greatly the effort required to generate that surface.

II. Methods

A. Electronic Structure Methods. The electronic structure of this system is quite complex and requires careful consideration. There are several asymptotes in the H−Cl + $O(^3P)$ reactive system These are composed of the three possible diatomic combinations and the three separated atoms. There are three separate transition structures (TS) along reaction paths

[†] Part of the "George C. Schatz Festschrift".

* Corresponding author: E-mail: jcamden@utk.edu and dawesr@missouri.edu.

10.1021/jp8113144 CCC: $40.75
Published on Web 03/06/2009

connecting three different pairs of association complexes. Treating the global configuration space within the C_s point group, the ground state triplet surface is of A'' symmetry. The ground $^3A''$ state is formally degenerate with the lowest $^3A'$ state at all linear and asymptotic configurations. Each of the asymptotes has different numbers of A' and A'' states contributing to the total number of degenerate states. The number of states in each case was derived from correlation tables given by Herzberg.[15] At the H−Cl, O−H, and O−Cl asymptotes there are degeneracy patterns of (1,2), (3,3), and (1,1) for the number of degenerate triplet states with (A',A'') symmetries, respectively. For the separated atoms a pattern of (8,10) makes up a total of 18 degenerate triplet states. Peterson et al.[16] constructed a very sophisticated high-level ab initio PES describing a single reaction channel for this system (connecting the H−Cl and O−H asymptotes). The ab initio calculations for that surface involved a state-averaged CASSCF (SA-CASSCF) reference used in a Davidson-corrected multireference configuration interaction (MRCI+Q) calculation. Due to the different degeneracy patterns at the two asymptotes, a dynamic weighting scheme (with an analytic functional form) was imposed on the SA-CASSCF reference calculation (DW-SA-CASSCF). This is designed to provide a smooth transition between correct electronic structures at the different asymptotes. Deskevich et al.[17] have developed an automatic, self-consistent dynamic-weighting scheme using the Molpro[18] electronic structure code. In this approach the weights are a function of the electronic level spacing and are determined self-consistently with an iterative series of DW-SA-CASSCF calculations.

Given the complexity of the global configuration space in this system (with a different degeneracy pattern at each of four asymptotes) we implemented the self-consistent dynamic weighting approach of Deskevich et al. Unfortunately, convergence issues arose in the ab initio calculations when all of the 18 states required to describe the global space of this system were included. We note that this difficulty is associated with the convergence of the electronic structure methods and not the IMLS fitting routine.

Rather than limit the configuration space of the fitted PES by excluding the separated atoms asymptote, we elected to use a hybrid-DFT method to compute a global PES. In previous studies of this system[10,11] by one of the authors a limited number of trajectories were performed using the UB3LYP/6-31G** and UMP2/cc-pVTZ methods. The B3LYP/6-31G** method was found to provide a physically realistic global surface but was limited in scope because of the cost associated with direct dynamics simulations. In that study about 3% of all trajectories failed due to lack of ab initio convergence at some point during the integration. These failures occurred despite using the converged orbitals at each time step as the initial guess for calculations at the next time step. This strategy does not always ensure convergence since the orbitals can change rapidly with respect to a particular coordinate. While it is certainly possible to implement other strategies during direct dynamics, the advantage of a fitted PES is that all of the convergence issues are dealt with in advance, and large numbers of trajectories can be run at low cost. We chose the UB3LYP/aug-cc-pVTZ method for our fitted PES. In another DFT-based study of this system, Hsiao et al.[19] report an additional A'' transition structure along the O + HCl → OH + Cl reaction channel. No corresponding structure has been identified at higher levels of theory. We found no such anomalies in our UB3LYP/aug-cc-pVTZ calculations. Due to convergence problems in the ab initio calculations for this system a grid of stored orbitals was set up to provide initial guesses for orbitals at geometries required by the IMLS automatic PES generation algorithm. Although the IMLS algorithm can often converge the fitting accuracy for three-atom PESs to high accuracy with only a few hundred points,[13] reliable ab initio convergence necessitated a denser grid in the present case. Prior to generating the IMLS PES, starting at a well-behaved geometry, orbitals were stored on a grid of 2196 points. The grid of stored orbitals was also generated automatically (using eight parallel processors) and then immediately interfaced with our IMLS fitting code. During the automatic PES generation, the calculation at each automatically determined geometry made use of the nearest stored orbitals (failing that, using the second or third nearest if necessary). This strategy was successful and ab initio calculations were reliably converged in all regions of the configuration space.

B. IMLS Fitted PES. An IMLS-based approach was used to fit a global PES by using the UB3LYP/aug-cc-pVTZ ab initio method and the Gaussian03[20] electronic structure code. The fitting was performed in internuclear distance coordinates with use of ab initio energy and analytic gradient data. Since the maximum energy of interest for this study was 6 eV, the fitted energy range was conservatively set to 6.25 eV (∼144 kcal/mol) above the O + HCl asymptote. The coordinate ranges were set to allow maximum internuclear distances of 8.0 Å. The minimum distances were determined by the energy range and were approximately 0.88, 1.24, and 0.65 Å for H−Cl, Cl−O, and O−H distances, respectively. As discussed in Section III.B, ab initio convergence required a dense grid of stored wave functions. Beginning with the grid of 2196 stored wave functions as initial data points the IMLS automatic surface generation algorithm was run in parallel on eight processors. A total of 232 additional automatically selected points (2428 points making up the complete data set) were added (eight points per iteration) before the estimated root-mean-square (rms) fitting error fell below our 0.1 kcal/mol accuracy target and a subroutine of the fitting parameters was output for use. The number of single point energy and gradient calculations required for the global surface is about the same as that required for only a single direct dynamics trajectory for this system, illustrating the significant computational savings.

C. Trajectory Calculations. The direct dynamics quasiclassical trajectory method applied to the O + HCl system is described elsewhere;[10] therefore, we only provide specific details for the present application here. Having a fitted global PES allowed a much more extensive study to be performed. The previous B3LYP direct dynamics study[11] was limited to batches of 900 trajectories (using the 6-31G** basis) at each energy. The IMLS method allowed an average of 435 energy and analytic gradient evaluations per second on our machines (2.4 GHz CPU). For the aug-cc-pVTZ basis set used in the fitted PES, this corresponds to a speedup factor of 66 729 over direct dynamics. Thus, batches of 10 000 quasiclassical trajectories were run at a variety of collision energies (E_{coll}) between 46 and 138 kcal·mol^{-1} to calculate reaction cross sections for the OH + Cl (σ_{OH}), OCl + H (σ_{OCl}), and O + H + Cl fragmentation (σ_{frag}) product channels. All calculations were performed on the ground triplet state surface ($^3A''$); we have discussed previously the possible contribution of the low-lying first excited triplet state ($^3A'$).[10] Trajectories are integrated by a standard fifth-order predictor, sixth-order corrector integration algorithm.[21] At each point along the trajectory the energy and gradient are obtained from the IMLS fitted PES, which was interfaced to our molecular dynamics code. The initial conditions were sampled randomly over orientations and the impact parameter. A single

TABLE 1: Two-Body Potentials: Dissociation Energies[a] (kcal/mol) and Bond Lengths[a] (Å), Compared with High-Level ab Initio and Experiment

	D_e	r_e
HCl		
UB3LYP/aug-cc-pVTZ	104.6	1.284
UB3LYP/6−31G**	103.1	1.286
MRCI+Q/CBS[b]	106.9	1.275
Experiment[c]	106.48	1.275
OH		
UB3LYP/aug-cc-pVTZ	108.0	0.975
UB3LYP/6-31G**	105.2	0.980
MRCI+Q/CBS[b]	106.2	0.968
experiment[c]	107.05	0.970
ClO		
UB3LYP/aug-cc-pVTZ	64.2	1.590
UB3LYP/6-31G**	59.8	1.620
MRCI+Q/CBS[b]	62.1	1.574
experiment[c]	64.64	1.570

[a] Computed from asymptotes on the three-atom PES. [b] Ramachandran and Peterson, ref 16. [c] Huber and Herzberg, ref 25, and Rucsic et al., ref 27 (including spin−orbit effects not treated here).

diatomic trajectory starting from the equilibrium HCl geometry is run with kinetic energy corresponding to the zero-point vibrational energy. The HCl vibrational phase for each reactive trajectory is then sampled randomly from the initial intramolecular trajectory. The maximum impact parameter, b_{max}, was 6.0 a_0 and is justified by examination of the resulting opacity functions. The integration time step is held constant at 5.0 au for all trajectories. Nearly perfect total energy conservation was obtained (better than 1×10^{-8} au), which is an improvement of about 3 orders of magnitude over the direct dynamics calculations reported earlier.[11] We attribute this improvement to the analytic gradients provided by the IMLS method on the fitted PES. Integration was terminated when the distance between any two atoms exceeded 10 au. We did not discard product trajectories with an internal energy below the harmonic zero point, as this can lead to an underestimation of the cross section.[22−24] When fragmentation occurs, the light H-atom often moves beyond the 10 au limit before the OCl breaks apart. In these cases we calculated the internal energy of the OCl product, and if it exceeded the threshold for fragmentation into Cl + O we assigned that trajectory to fragmentation.

III. Results and Discussion

A. Fitted Potential Energy Surface. In Table 1 the three calculated diatomic equilibrium bond distances and dissociation energies are compared to the results of high-level ab initio calculations and experiment.[16,25] The performance of the smaller 6-31G** basis used in previous direct dynamics studies[10,11] is also compared. The diatomic energies and equilibrium bond distances were evaluated in the fitted three-atom configuration space (fixing two internuclear distances at the maximum fitted distance of 8 Å, while optimizing the third). Dissociation energies of the diatomics are reported relative to the O + H + Cl asymptote (where all three internuclear distances are 8 Å). The aug-cc-pVTZ basis set produces a significant improvement over the 6-31G** basis for the calculated dissociation energies. The relatively low-cost UB3LYP method (not including spin orbit effects) produces good (and likely fortuitous) agreement with experiment. The mean error compared with experiment was reduced from 3.36 kcal/mol to only 1.09 kcal/mol. This is even better than the MRCI+Q/CBS method, which has a mean error of 1.27 kcal/mol. These values determine the accuracy of the overall energy changes associated with each reaction channel. Calculated equilibrium bond distances (minima on the potential) were also significantly improved with the larger basis set. The maximum error relative to experiment was reduced from 0.05 Å (ClO, UB3LYP/6-31G**) to 0.02 Å (ClO, UB3LYP/aug-cc-pVTZ). The MRCI+Q/CBS results are much better with a maximum error of 0.004 Å.

Table 2 lists the relative energies and geometric parameters for structures along each reaction path. Reaction path 1 is the O + HCl → OH + Cl channel. The barrier to this low-energy

TABLE 2: Relative Energies (kcal/mol) of Asymptotes,[a] Transition Structures,[b] and van der Waals Complexes for the Three Reaction Paths

Reaction Path 1: O + HCl → OH + Cl				
structure	ΔV (kcal/mol)	r_{HCl}	r_{OH}	θ_{OHCl}
O + HCl	0.00	1.284	8.000	
O−HCl	−1.64	1.290	2.165	180.00
O−H−Cl (TS 1)	2.11	1.398	1.338	139.28
OH−Cl	−15.02	2.417	0.976	62.27
OH + Cl	−3.45	8.000	0.975	
Reaction Path 2: O + ClH → OCl + H				
structure	ΔV (kcal/mol)	r_{HCl}	r_{OCl}	θ_{OClH}
O + ClH	0.00	1.284	8.000	
O−ClH	−1.05	1.284	2.795	79.81
O−Cl−H (TS 2)	40.81	2.090	1.612	158.61
OCl−H	40.17	2.803	1.593	177.31
OCl + H	40.39	8.000	1.590	
Reaction Path 3: Cl + OH → ClO + H				
structure	ΔV (kcal/mol)	r_{ClO}	r_{OH}	θ_{ClOH}
Cl + OH	−3.45	8.000	0.975	
Cl−OH	−15.02	2.144	0.976	93.95
Cl−O−H (TS 3)	43.71	1.648	1.655	147.26
ClO−H	40.33	1.591	3.028	116.69
ClO + H	40.39	1.590	8.000	

[a] All energies relative to O + HCl asymptote. [b] Imaginary frequencies for TS 1, 2, and 3 are respectively 908i, 410i, and 931i cm^{-1}.

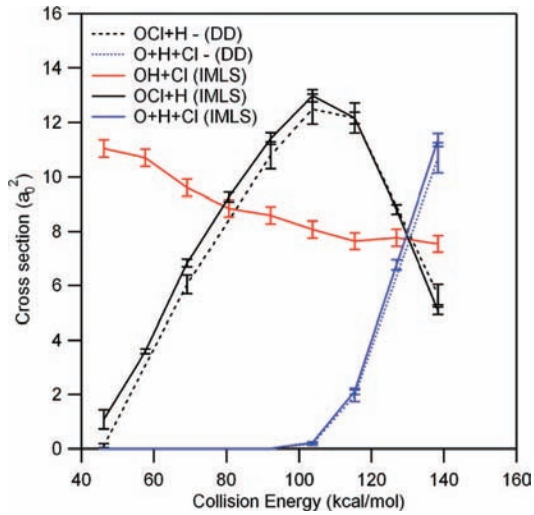

Figure 1. Theoretical excitation functions for the O + HCl → OH + Cl (red), O + HCl → OCl + H (black), and O + HCl → O + H + Cl (blue) reactions calculated on the IMLS B3LYP/aug-cc-pVTZ fitted surface. Direct dynamics calculations at the B3LYP/6-31G** level are from ref 10 (dotted curves).

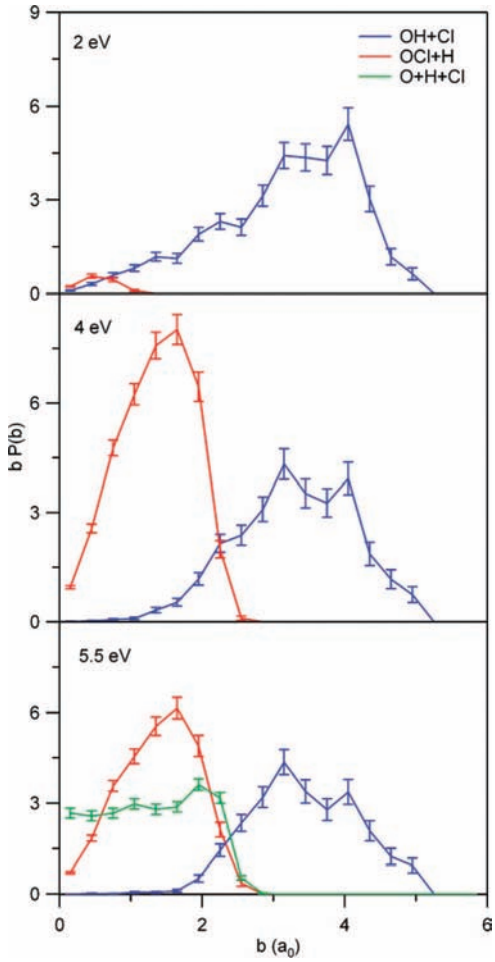

Figure 2. Opacity functions, plotted as $bP(b)$, for the O + HCl → OH + Cl (blue), O + HCl → OH + Cl (red), and O + HCl → O + H + Cl (green) reactions at center of mass collision energies between 2 and 6 eV. The area under each curve is equal to the reaction cross section in a_0^2 for the particular channel in question.

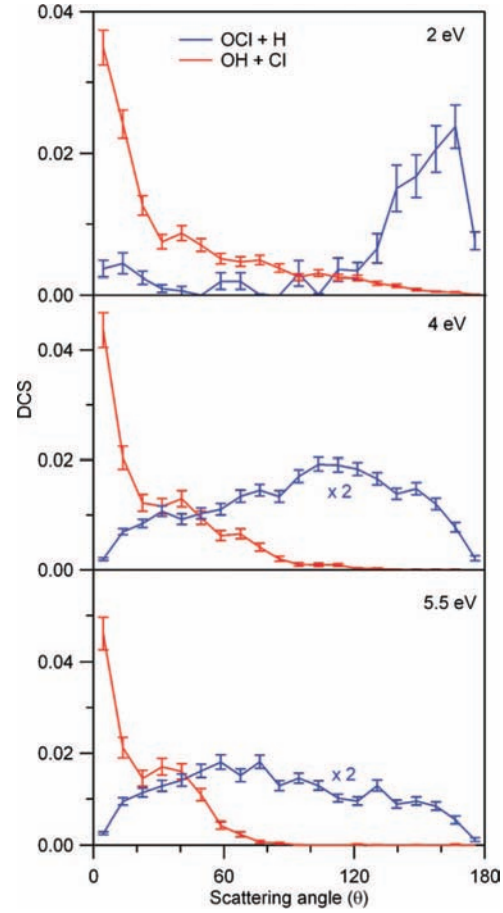

Figure 3. Differential cross sections plotted for the O + HCl → OH + Cl (blue), O + HCl → OH + Cl (red), and O + HCl → O + H + Cl (green) reactions at center of mass collision energies between 2 and 6 eV. Scattering angle refers to the molecular product (OCl or OH) and $\theta = 0$ is forward scattering relative to the initial O-atom velocity vector. All distributions are normalized to unity.

channel is poorly represented by the B3LYP method. The calculated barrier height is only 2.11 kcal/mol. Various high-level calculations estimate a barrier of at least 10 kcal/mol.[16] Despite this difference, geometric parameters at the transition structure (TS) are similar to those obtained at higher levels. Also, the product side van der Waals complex is more stable than predictions by high-level methods, and the overall energy change (without zero-point corrections) is somewhat greater (−3.45 kcal/mol) than experiment (−0.57 kcal/mol). The higher energy channels are better described, with barrier heights in closer agreement with high-level methods, and overall energy changes in better agreement with experiment. The overall energy change for the O + ClH → OCl + H reaction is 40.39 kcal/mol compared to 41.84 kcal/mol from experiment (see Table 1). While dynamics at low collision energies, i.e., those where the OCl + H and O + H + Cl channels are closed, will not be well-described by our current surface, the B3LYP method provides a physically realistic global PES especially for the high-energy reactions including complete dissociation. The availability of analytic gradients at relatively low cost was also advantageous for use with the IMLS automatic surface generation method.

B. Trajectory Calculations. The reaction cross sections for the OH + Cl, OCl + H, and O + H + Cl reaction channels on the B3LYP/aug-cc-pVTZ IMLS fitted surface are displayed in Figure 1. These are compared to the previous direct dynamics results for the OCl + H and O + H + Cl channels with the smaller UB3LYP/6-31G(d,p) basis set. There is good agreement between the results of the current study and experimental results.[11] The shapes of the OCl + H and O + H + Cl excitation functions have been described previously[10,11] and are attributed to the relative importance of two distinct dynamical mechanisms for OCl + H formation.

The OH + Cl channel was not examined in the previously reported B3LYP/6-31G** direct dynamics study[11] due to the computational cost associated with sampling the large range of impact parameters required to study that channel. This cost arises because b_{max} for OCl + H is significantly smaller than b_{max} for OH + Cl (see Figure 2); therefore, if a large value of b_{max} is used, many fewer OCl reactive trajectories result for the same computational effort. In the previous study, we chose to focus on the OCl + H channel at the expense of obtaining information on the OH + Cl channel. By using the IMLS-fitted surface developed here many more trajectories could be run, and thus it was feasible to include that channel in the study. The OH + Cl channel slowly decreases as the collision energy is increased, a feature often observed for abstraction reactions that proceed via a stripping mechanism.[26]

Figure 2 displays opacity functions, plotted as $bP(b)$, for the OH + Cl, OCl + H, and O + H + Cl reactive channels. The formation of OH is favored for large values of b at all collision energies and $P(b)$ is relatively unchanged as the collision energy is increased. The formation of OCl is favored by small impact

parameters. The fragmentation channel is also favored at small impact parameters but interestingly b_{max} for fragmentation is very similar to the observed b_{max} for OCl formation. This occurs because the fragmentation mechanism is a two-step process in the energy range that was studied. Initially O and HCl react to form OCl and H; however, depending on the collision geometry the kinetic energy of the H-atom can be limited while the OCl internal energy exceeds the dissociation energy. This situation results in fragmentation into three atoms. The geometric requirements of this mechanism were recently discussed in terms of the asymptotic angle between the O-atom velocity vector and HCl bond axis in the reagent valley.[11]

Figure 3 displays differential cross sections for the OH and OCl products as a function of collision energy. Over the studied energy range the OH product is scattered into the forward hemisphere, where forward ($\theta = 0$) is defined with respect to the incident O atom velocity vector. The OCl product is mainly backward scattered near the threshold but becomes more isotropic as the collision energy increases.

IV. Summary

We have performed a comprehensive quasiclassical trajectory study of the O + HCl reactive system for collision energies between 46 and 138 kcal/mol on a global potential energy surface. Reaction cross sections, opacity functions, and differential cross sections for all open product channels were calculated. The current trajectory study improves on previous direct dynamics simulations by eliminating many of the drawbacks of that approach, such as trajectory failure due to lack of convergence of the ab initio calculations, relatively poor energy conservation during trajectories, the severe limitations on the level of ab initio theory that is feasible to use, and numbers of trajectories that can be computed. These results demonstrate that IMLS provides an economical method to generate global PESs for systems with multiple reaction channels.

Acknowledgment. This work was supported by the U.S. Department of Energy, Office of Basic Energy Sciences, Division of Chemical Sciences, under Contract No. DE-FG02-01ER15231 (R.D. and D.L.T), and the University of Tennessee, Knoxville (J.P.C.). R.D. thanks Kirk Peterson, Larry Harding, and Mike Deskevich for useful discussions about high-level electronic structure methods.

References and Notes

(1) Dressler R. E. *Chemical Dynamics in Exytreme Environments*; World Scientific: Singapore, 2001; Vol. 11.
(2) Fogarty, D. P.; Kandel, S. A. *J. Chem. Phys.* **2006**, *124*, 111101.
(3) Gibson, K. D.; Isa, N.; Sibener, S. J. *J. Phys. Chem. A* **2006**, *110*, 1469.
(4) Brunsvold, A. L.; Zhang, J. M.; Upadhyaya, H. P.; Minton, T. K.; Camden, J. P.; Paci, J. T.; Schatz, G. C. *J. Phys. Chem. A* **2007**, *111*, 10907.
(5) Tasic, U. S.; Yan, T. Y.; Hase, W. L. *J. Phys. Chem. B* **2006**, *110*, 11863.
(6) Gimelshein, S. F.; Levin, D. A.; Alexeenko, A. A. *J. Spacecr. Rockets* **2004**, *41*, 582.
(7) Murad, E. *J. Spacecr. Rockets* **1996**, *33*, 131.
(8) Troya, D.; Schatz, G. C. *Int. Rev. Phys. Chem.* **2004**, *23*, 341.
(9) Garton, D. J.; Brunsvold, A. L.; Minton, T. K.; Troya, D.; Maiti, B.; Schatz, G. C. *J. Phys. Chem. A* **2006**, *110*, 1327.
(10) Camden, J. P.; Schatz, G. C. *J. Phys. Chem. A* **2006**, *110*, 13681.
(11) Zhang, J. M.; Camden, J. P.; Brunsvold, A. L.; Upadhyaya, H. P.; Minton, T. K.; Schatz, G. C. *J. Am. Chem. Soc.* **2008**, *130*, 8896.
(12) Dawes, R.; Thompson, D. L.; Guo, Y.; Wagner, A. F.; Minkoff, M. *J. Chem. Phys.* **2007**, *126*, 184108.
(13) Dawes, R.; Thompson, D. L.; Wagner, A. F.; Minkoff, M. *J. Chem. Phys.* **2008**, *128*, 084107.
(14) Guo, Y.; Tokmakov, I.; Thompson, D. L.; Wagner, A. F.; Minkoff, M. *J. Chem. Phys.* **2007**, *127*, 214106.
(15) Herzberg, G. *Molecular Spectra and Molecular Structure: I−III*; Prentice-Hall, Inc.: New York, 1939−1966.
(16) Ramachandran, B.; Peterson, K. A. *J. Chem. Phys.* **2003**, *119*, 9590.
(17) Deskevich, M. P.; Nesbitt, D. J.; Werner, H. J. *J. Chem. Phys.* **2004**, *120*, 7281.
(18) *MOLPRO,* a package of ab initio programs, written by: Werner, H.-J.; Knowles, P. J.; Lindh, R.; Manby, F. R.; Schütz, M.; Celani, P.; Korona, T.; Rauhut, G.; Amos, R. D.; Bernhardsson, A.; Berning, A.; Cooper, D. L.; Deegan, M. J. O.; Dobbyn, A. J.; Eckert, F.; Hampel, C.; Hetzer, G.; Lloyd, A. W.; McNicholas, S. J.; Meyer, W.; Mura, M. E.; Nicklaβ, A.; Palmieri, P.; Pitzer, R.; Schumann, U.; Stoll, H.; Stone, A. J.; Tarroni, R.; Thorsteinsson, T.
(19) Hsiao, C. C.; Lee, Y. P.; Want, N. S.; Wang, J. H.; Lin, M. C. *J. Phys. Chem. A* **2002**, *106*, 10231.
(20) Frisch, M. J.; Trucks, G. W.; Schlegel, H. B.; Scuseria, G. E.; Robb, M. A.; Cheeseman, J. R.; Montgomery, J. A., Jr.; Vreven, T.; Kudin, K. N.; Burant, J. C.; Millam, J. M.; Iyengar, S. S.; Tomasi, J.; Barone, V.; Mennucci, B.; Cossi, M.; Scalmani, G.; Rega, N.; Petersson, G. A.; Nakatsuji, H.; Hada, M.; Ehara, M.; Toyota, K.; Fukuda, R.; Hasegawa, J.; Ishida, M.; Nakajima, T.; Honda, Y.; Kitao, O.; Nakai, H.; Klene, M.; Li, X.; Knox, J. E.; Hratchian, H. P.; Cross, J. B.; Bakken, V.; Adamo, C.; Jaramillo, J.; Gomperts, R.; Stratmann, R. E.; Yazyev, O.; Austin, A. J.; Cammi, R.; Pomelli, C.; Ochterski, J. W.; Ayala, P. Y.; Morokuma, K.; Voth, G. A.; Salvador, P.; Dannenberg, J. J.; Zakrzewski, V. G.; Dapprich, S.; Daniels, A. D.; Strain, M. C.; Farkas, O.; Malick, D. K.; Rabuck, A. D.; Raghavachari, K.; Foresman, J. B.; Ortiz, J. V.; Cui, Q.; Baboul, A. G.; Clifford, S.; Cioslowski, J.; Stefanov, B. B.; Liu, G.; Liashenko, A.; Piskorz, P.; Komaromi, I.; Martin, R. L.; Fox, D. J.; Keith, T.; Al-Laham, M. A.; Peng, C. Y.; Nanayakkara, A.; Challacombe, M.; Gill, P. M. W.; Johnson, B.; Chen, W.; Wong, M. W.; Gonzalez, C.; Pople, J. A. *Gaussian 03*; Gaussian, Inc., Wallingford, CT, 2004.
(21) Press, W. H.; Flannery, B. P.; Teukolsky, S. A.; Vetterling, W. T. *Numerical Recipes in FORTRAN: The Art of Scientific Computing*, 2nd ed.; Cambridge University Press: Cambridge, England, 1992.
(22) Dong, E. J.; Setser, D. W.; Hase, W. L.; Song, K. *J. Phys. Chem. A* **2006**, *110*, 1484.
(23) Kumar, S.; Sathyamurthy, N.; Ramaswamy, R. *J. Chem. Phys.* **1995**, *103*, 6021.
(24) Troya, D.; Lakin, M. J.; Schatz, G. C.; Gonzalez, M. *J. Chem. Phys.* **2001**, *115*, 1828.
(25) Huber, K. P.; Herzberg, G. *Molecular Spectra and Molecular Structure: IV. Constants of Diatomic Molecules*; Van Nostrand Reinhold: New York, 1979.
(26) Camden, J. P.; Hu, W. F.; Bechtel, H. A.; Brown, D. J. A.; Martin, M. R.; Zare, R. N.; Lendvay, G.; Troya, D.; Schatz, G. C. *J. Phys. Chem. A* **2006**, *110*, 677.
(27) Ruscic, B.; Wagner, A. F.; Harding, L. B.; Asher, R. L.; Feller, D.; Dixon, D. A.; Peterson, K. A.; Song, Y.; Qian, X. M.; Ng, C. Y.; Liu, J. B.; Chen, W. W. *J. Phys. Chem. A* **2002**, *106*, 2727.

JP8113144